Contents list available at CBIORE journal website

International Journal of Renewable Energy Development

Journal homepage: https://ijred.cbiore.id

Research Article

Light intensity enhances fatty acid and biomass composition of an acidophilic *Euglena gracilis* isolated from Dieng peatland, Central Java for biofuel production

David Aritonang[a*], Tia Erfianti[b], Renata Adaranyssa Egistha Putri [c], Kartina[a,d], Shela Delfia Ramadhana[a], Brilian Ryan Sadewo[e,f], Angga Puja Asiandu[a], Eko Agus Suyono[a,f*]

[a] *Faculty of Biology, Universitas Gadjah Mada, Jl. Teknika Selatan, Sleman 55281, Yogyakarta, Indonesia*

[b] *Postdoctoral Program, National Research and Innovation Agency, Gunungkidul, 55861, Indonesia*

[c] *Study Program of Biotechnology, Graduate School of Universitas Gadjah Mada, Yogyakarta, 55281, Indonesia*

[d] *Study Program of Aquaculture, Faculty of Fisheries and Marine Sciences, Universitas Borneo Tarakan, North Kalimantan, 77115, Indonesia*

[e] *Department of Civil and Environmental Engineering, Universitas Gadjah Mada, Jl. Grafika 2 Yogyakarta 55281, Indonesia*

[f] *Center of Excellent for Microalgae Biorefinery, Universitas Gadjah Mada, Sleman 55281, Yogyakarta, Indonesia*

Abstract. Optimizing environmental factors in microalgal cultivation is essential for improving biomass and lipid production for biofuel applications. This study examined the effects of light intensity under 15% CO_2 supplementation on growth, biomass, lipid and paramylon productivity, pigment content, and fatty acid methyl ester (FAME) composition in a local acidophilic *E. gracilis* strain cultivated at 500, 2,100, 4,500, 6,000, and 8,500 lux. The highest proportions of saturated, monounsaturated, and polyunsaturated fatty acids were observed at 8,500 lux (42.35%), 500 lux (59.01%), and 4,500 lux (23.705%), respectively. Methyl palmitoleate (C16:1) showed its highest relative abundance at 500 lux (32.46%), whereas its relative abundance at 6,000 lux was 26.34%. Biomass and lipid productivities were highest at 6,000 lux (0.0874 ± 0.0035 and 0.0311 ± 0.0030 mg/mL/day, respectively), while paramylon productivity was highest at 8,500 lux (0.030 ± 0.0011 mg/mL/day). The logistic growth model gave the highest maximum specific growth rate at 8,500 lux (0.78 day^{-1}). Chlorophyll a, chlorophyll b, and carotenoid contents peaked at 6,000 lux. The predicted biodiesel properties at 6,000 lux were an iodine value of 89.67 g I_2/100 g, a saponification value of 190.99 mg KOH/g, and a cetane number of 49.16. Overall, 6,000 lux provided the best balance for biomass and lipid production, whereas 8,500 lux favored paramylon accumulation. The FAME profile, particularly the high relative abundance of C16:1, supports further evaluation of this strain as a biodiesel feedstock.

Keywords: bioenergy, biorefinery, *E. gracilis*, FAMEs, microalgae biomass

Received: 4th Sept 2025; Revised: 7th March 2026; Accepted: 18th August 2026; Available online: 20th Sept 2026

1. Introduction

The industrial revolution of the 21st century has contributed to a 32% increase in CO_2 concentrations over the past 50 years (Herzog *et al.,* 2000). This increase is associated with population growth and rising global energy demand. Global CO_2 emissions reached 36.7 Gt in 2019, declined to 34.8 Gt during the COVID-19 pandemic in 2020, and increased again to 36.4 Gt in 2021 (Friedlingstein *et al.,* 2022). Biofuel offers an alternative for addressing energy scarcity and reducing global fossil fuel emissions (Singh *et al.,* 2022). First-generation biofuel is derived from biomass that competes with food production, while second-generation biofuel is produced from cellulose. Third-generation biofuel is derived from algae, whereas fourth-generation biofuel is produced from genetically modified organisms (Shokravi *et al.,* 2022). However, bioenergy production using first- and second-generation biomass creates social and environmental sustainability problems. These problems include deforestation, changes in land prices, and increased conflicts of interest within society (Papilo *et al.,* 2022).

Microalgae are a suitable renewable energy source without the drawbacks associated with first- and second-generation biofuels (Sathya *et al.,* 2023). They produce environmentally friendly biofuel through sustainable lipid synthesis (Song *et al.,* 2023). They can also reduce carbon dioxide emissions because their CO_2 fixation rates are 10 to 50 times higher than those of terrestrial plants (Onyeaka *et al.,* 2021). Other advantages of this sustainable biomass include a short generation cycle, rapid reproduction, and greater accumulation of targeted molecules (Song *et al.,* 2023). However, microalgal growth is affected by environmental factors such as temperature and pH (Wang *et al.,* 2018). In particular, optimal temperature is one of the main abiotic factors influencing microalgal growth (Metsoviti *et al.,* 2019).

One promising microalga is *Euglena gracilis*, a unicellular photosynthetic organism that lacks a cell wall. This strain has

* Corresponding author
Email: davidaritonangraja@gmail.com (D. Aritonang); eko_suyono@ugm.ac.id (E.A. Suyono)

https://doi.org/10.61435/ijred.2026.61637
ISSN: 2252-4940/© 2026.The Author(s). Published by CBIORE

chloroplasts that enable it to conduct photosynthesis (Wardana *et al.,* 2023). *E. gracilis* has considerable potential for bioenergy production because it produces lipids that can be converted into biodiesel (Nur *et al.,* 2023). It can be cultivated under photoautotrophic, heterotrophic, and mixotrophic conditions during its life cycle. It also contains valuable bioproducts, including essential amino acids, vitamins, lipids, and the β-1,3-glucan paramylon (Gissibl *et al.,* 2019). Moreover, *E. gracilis* is rich in polyunsaturated fatty acids (PUFAs), which are valuable to the biorefinery industry for producing environmentally friendly biodiesel (Uliesther *et al.,* 2023). This acid-tolerant microalga can grow at pH 3 (Kitaya *et al.,* 2005). It can also use sunlight as its primary energy source while utilizing CO_2, water, and mineral salts to produce carbohydrates and biomass (Sathya *et al.,* 2023).

Optimal environmental conditions are essential for maximizing yields in microalgal cultivation. One critical factor is light intensity, which can limit the growth of microalgae as photosynthetic organisms. Exposure to optimal light intensity enhances microalgal growth, biomass, and metabolite production, whereas inadequate or excessive light reduces cell productivity (Carvalho *et al.,* 2011). For instance, *Chlorella vulgaris*, *C. sorokiniana,* and *C. reinhardtii* grew slowly under 30-50 µmol photons. When the light intensity increased to 150-200 µmol photons, the growth of all three strains increased significantly (Ievina & Romagnoli 2020). Meanwhile, *E. gracilis* is an actively motile strain that is sensitive to light intensity and exhibits positive and negative phototactic responses (Ozasa *et al.,* 2019). Light exposure also strongly influences its growth, fatty acid composition, biomass accumulation, and biomass components, including lipids, proteins, carbohydrates, and pigments (Constantopoulos & Bloch 1967; Erfianti *et al.,* 2024a). Therefore, appropriate light intensity is essential for *Euglena* cultivation (Ozasa *et al.,* 2019).

Light intensity also plays an important role in microalgal lipid synthesis. High light intensity causes photooxidation in cells. To protect themselves, cells accumulate more lipids by converting excess photoassimilates into fatty acids (Nzayisenga *et al.,* 2020; Solovchenko 2012). A previous study found that lipid accumulation in *Desmodesmus* sp. and *S. obliquus* increased as light intensity rose to 300 µmol photons m^{-2} s^{-1}. Higher light intensity also increased the accumulation of oleic acid (18:1) (Nzayisenga *et al.,* 2020). Phototrophically cultured *E. gracilis* produced higher levels of total unsaturated fatty acids, omega-3, and α-tocopherol than cultures grown in the dark. Under light exposure, it accumulated 12-34% protein and more than 0.15 µg/mg paramylon (Wang *et al.,* 2018).

Furthermore, CO_2 concentration influences biomass productivity and secondary metabolite production in *E. gracilis* (Yadav *et al.,* 2013). A previous study reported that the CO_2 fixation rates of *E. gracilis* at 400 ppm and CO_2 concentrations of 6%, 15%, 60%, and 99% were 0.018, 0.234, 0.040, and 0.004 mg/mL/h, respectively (Xin *et al.,* 2023). Another study found that CO_2 increased the expression of genes involved in photosynthesis and sugar metabolism in *Euglena* sp. (Yuan *et al.,* 2024). Enrichment with 15% CO_2 was also reported to increase lipid accumulation in this strain by 0.35 g/L (Erfianti *et al.,* 2024b).

Although the effects of light and CO_2 supplementation on *Euglena* species have been widely investigated, previous studies have focused mainly on biomass growth, metabolite accumulation, and carbon sequestration. In the acidophilic *Euglena gracilis* strain isolated from Dieng Peatland, photoperiod regulation, nutrient manipulation, light spectrum, and CO_2 supplementation influence biomass productivity, lipid accumulation, pigment composition, paramylon biosynthesis, wax ester production, and carbon capture efficiency (Erfianti *et al.,* 2024a; Erfianti *et al.,* 2024b; Erfianti *et al.,* 2024c; Ramadhana *et al.,* 2025). However, the combined effects of irradiance and elevated CO_2 on carbon partitioning between lipid and paramylon storage remain poorly understood. Limited information is also available on how these metabolic shifts affect fatty acid composition and biofuel feedstock quality. Therefore, this study investigated the effects of different light intensities (500-8500 lux) under 15% CO_2 supplementation on biomass production, lipid and paramylon accumulation, and fatty acid composition in an acidophilic *Euglena gracilis* strain. Particular attention was given to irradiance-driven carbon partitioning between lipid and paramylon storage and its implications for fatty acid profiles and biofuel feedstock quality.

2. Materials and Methods

2.1 Strain and culture conditions

The *E. gracilis* strain used in this study was isolated from Dieng Peatland, Central Java, Indonesia, and identified by Erfianti *et al.* (2024a). The strain was cultivated in CM medium (Cramer & Myers 1952). The initial pH was adjusted to 3.5, the optimal acidity level for *E. gracilis*. For subculturing, 200 mL of *E. gracilis* starter culture was mixed with 800 mL of sterilized Cramer and Myers medium. The flask was tightly covered with cotton, connected to an aeration hose, and placed in a cultivation room under a 24:0 photoperiod. The cultures were exposed to light intensities of 500, 2,100, 4,500, 6,000, and 8,500 lux. During the 15-day cultivation period, all treatments received continuous aeration with a gas mixture of 15% CO_2 and 85% ambient air at a flow rate of 0.8 liters per minute (LPM). The pH was not treated as an independent variable and was not monitored or readjusted during cultivation. A low initial pH was used because *Euglena* grows well under acidic conditions (Suzuki, 2017).

2.2 Cell density measurement

Cell density was measured daily throughout the lag, exponential, stationary, and death phases. Cells were counted using a hemocytometer and a hand counter under an Olympus CX22LED microscope at 40× magnification. Cell density was calculated using the following formula (Indahsari *et al.,* 2022):

$$\text{Cell density (Cell/mL)} = \frac{\text{Counted cell quantity}}{4} \times 10^4 \quad (1)$$

2.3 Growth kinetics modeling

Microalgal growth is affected by environmental factors such as light intensity, temperature, pH, and nutrient sources. The growth rate of microalgae can be predicted using growth kinetic modeling (Krichen *et al.,* 2021). The growth kinetics of *E. gracilis* were analyzed using logistic and Gompertz models to predict cell density and the maximum daily growth rate. The logistic model was calculated using the following equations, where X is cell density, X_0 is the initial cell density, X_{max} is the maximum cell density, and μ_{max} is the maximum specific growth rate (Hanief *et al.,* 2020; Phukoetphim *et al.,* 2017).

$$\frac{dx}{dt} = \mu_{max}\left(1 - \frac{x}{X_{max}}\right) x \quad (2)$$

$$X = \frac{x_0 \, exp\,(\mu_{max} t)}{1-\left[\frac{x}{x_{max}}(1-exp\,(\mu_{max} t))\right]} \quad (3)$$

The Gompertz model was also used to estimate the population during the exponential phase. Its parameters included the relative maximum cell production rate (r_m) and lag time (t_L). The Gompertz model was calculated using the following equation:

$$x = X_0 + \left[X_{max} \, . \, exp\left[-exp\left(\left(\frac{r_m . \exp(1)}{X_{max}}\right)(t_L - t) + 1\right)\right]\right] \quad (4)$$

Model fit was determined using the following equation, where SSR is the sum of squared residuals and SST is the total sum of squares (Hanief *et al.,* 2020; Phukoetphim *et al.,* 2017).

$$R^2 = \left(1 - \frac{SSR}{SST}\right) \quad (5)$$

The Richards model was also used to determine growth kinetics with more complex parameters:

$$y = A\,(1 + v\exp(1+v) exp\,(\frac{\mu m}{A}(1+v)(1+\frac{1}{v})(tl - t))^{(-1/v)} (6)$$

Here, A is the asymptotic value of ln X_t/X_o, t is the residence time in days, v and k are shape parameters, and τ is the time at the inflexion point (Lam *et al.,* 2017).

2.4 Chlorophyll and carotenoid estimation

Chlorophyll a, chlorophyll b, and carotenoid contents were determined on days 0, 3, 6 and 9. A 2 mL sample was centrifuged at 4,000 rpm for 10 minutes. The pellet was extracted with 2 mL of methanol, covered with aluminum foil, and incubated for 24 hours (Pruvost *et al.,* 2011). Absorption spectra were recorded from 400 to 750 nm. Chlorophyll a (Chl a), chlorophyll b (Chl b), and carotenoid contents were calculated using the following formulas (Bogue *et al.,* 1957; Ritchie 2006):

[Chl a] μg/mL = - 8.0962 × A_{652} + 16.5169 × A_{665}

[Chl b] μg/mL = 27.4405 × A_{652} – 12.1688 × A_{665}

[Carotenoids] μg/mL = 4 × A_{480} (7)

2.5 Biomass analysis

Biomass measurements were performed on days 0, 3, 6, and 9. Samples were collected in 10 mL conical tubes under laminar airflow, shaken, and filtered using vacuum filtration and filter paper. The filter paper containing *E. gracilis* biomass was dried in an oven at 90°C for 30 to 60 minutes to obtain the net weight. The final weight of the filter paper and biomass was then measured using an analytical balance (Olguín *et al.,* 2015). The net biomass weight was calculated using the following formula (Husna *et al.,* 2020),

$$Biomass\,(\frac{mg}{mL}) = \frac{b-a}{c} \quad (8)$$

Here, a is the initial weight of the filter paper, b is the final weight of the filter paper and sample, and c is the sample volume. Net biomass productivity was calculated using the following formula (Nurafifah *et al.,* 2023):

$$Productivity\ of\ Biomass = \left(\frac{mg}{mL}\ /day\right) = \frac{\Delta x}{t} \quad (9)$$

Here, Δx is the change in biomass between days t_1 and t_0, and t is the time interval in days.

2.6 Lipid content analysis

Lipid content was measured on cultivation days 0, 3, 6, and 9. A 10 mL sample was centrifuged at 4,000 rpm for 10 minutes. The pellet was extracted by adding methanol and chloroform at a ratio of 2:1. The mixture was then centrifuged at 4,000 rpm for 10 minutes. After three layers formed, the bottom layer was transferred to a preweighed Petri dish (Bligh and Dyer, 1959). Total lipid content was calculated using the following formula (Nurafifah *et al.,* 2023):

$$Total\ Lipid\ \left(\frac{mg}{mL}\right) = \frac{final\ sample\ weight - initial\ sample\ weight}{Volume} \quad (10)$$

Lipid productivity was calculated using the following formula:

$$Lp\,(\frac{mg}{mL}/day) = Pdwt\ \times\ Lc \quad (11)$$

Here, Lp is lipid productivity (mg/mL/day), *Pdwt* is biomass productivity, and Lc is lipid content (Praharyawan *et al.,* 2016).

2.7 Carotenoid derivatives

Carotenoid derivatives were measured on days 0, 3, 6, and 9. A 5 mL sample of *E. gracilis* was centrifuged at 4,000 rpm for 10 minutes. The pellet was then extracted with either 90% ethanol or 90% acetone and incubated at 4°C for 24 hours. The samples were analyzed using a spectrophotometer, with absorbance coefficients based on (Thrane *et al.,* 2015).

2.8 Paramylon analysis

Paramylon was measured on days 0, 3, 6, and 9. A 20 mL sample was centrifuged at 4,000 rpm for 5 minutes. The pellet was treated with 500 μL of 1% sodium dodecyl sulfate (SDS) and 500 μL of 5% Na_2EDTA, then incubated in a water bath at 37°C for 30 minutes. The mixture was centrifuged at 4,000 rpm for 10 minutes and washed three times with sterile distilled water (Barsanti *et al.,* 2001). Paramylon content was measured using the Dubois method (Dubois *et al.,* 1951). The extracted solution was mixed with 500 μL of 5% phenol and 500 μL of H_2SO_4, then incubated for approximately 30 minutes. Absorbance was measured at 480 nm using a spectrophotometer. The blank contained 500 μL of 5% phenol and 500 μL of H_2SO_4.

2.9 Fatty acid analysis

Fatty acids were analyzed as fatty acid methyl esters (FAMEs) using gas chromatography with a flame ionization detector (GC-FID) at the LPPT Research Laboratory, Universitas Gadjah Mada. The analysis followed a two-stage hydrolysis and methylation procedure (Young *et al.,* 2012). For hydrolysis, 5 g of *E. gracilis* biomass from each light intensity treatment was mixed with 10 mL of concentrated HCl and heated at 80°C for 3 h. After cooling, the hydrolysate was extracted with 25 mL of a 1:1 (v/v) mixture of diethyl ether and petroleum ether. The upper organic layer was collected and evaporated under nitrogen. For methylation, 0.5 mL of the lipid extract was mixed with 1.5 mL of sodium methoxide solution

and heated at 60°C for 5-10 min with intermittent shaking. After cooling, 2 mL of boron trifluoride methanol reagent was added, and the mixture was reheated at 60°C for 5-10 min. The resulting FAMEs were extracted with 1 mL of heptane and 1 mL of saturated NaCl solution. The upper phase was transferred to a GC vial, and 1 µL was injected into an Agilent Technologies 7890B GC-FID system.

FAMEs were identified by comparing sample retention times with those of the reference FAME standards used by the analytical laboratory. Because GC-FID rather than GC-MS was used, mass spectral library matching and similarity index thresholds were not applicable. The relative abundance of each detected FAME was calculated from its peak area as a percentage of the total identified FAME peak area. Thus, the chromatograms provided evidence of peak separation and identification was based on retention time, whereas definitive structural confirmation using mass spectra was beyond the scope of this analysis.

Biodiesel quality parameters were estimated from the FAME profiles obtained by GC-FID using established empirical correlations (Klopfenstein, 1985; Gopinath *et al*., 2009; Mekonnen *et al*., 2024).

2.10 Iodine value (IV, g I_2/100 g)

The IV represents the degree of unsaturation and was calculated as follows:

$$IV = \sum_{i=1}^{n} \left(\frac{254 \times DB_i \times \%FA_i}{MW_{FA_i}} \right) \quad (12)$$

where DB_i is the number of double bonds, $\%FA_i$ is the mass percentage, and MW_{FA_i} is the molecular weight (g/mol) of fatty acid methyl ester *i*. Saturated FAMEs contribute zero to the IV.

2.11 Saponification value (SV, mg KOH/g)

The SV reflects average molecular weight and was calculated as follows:

$$SV = \sum_{i=1}^{n} \left(\frac{560 \times \%FA_i}{MW_{FA_i}} \right) \quad (13)$$

where 560 is the conversion factor (560 ≈ 56 × 10; 56 = molecular weight of KOH).

2.12 Cetane number (CN)

The CN, which indicates ignition quality, was predicted using the Klopfenstein equation:

$$CN = 46.3 + \frac{545}{SV} + \frac{0.225}{IV} \quad (14)$$

Molecular weights and double bond counts were assigned based on standard FAME structures. Calculations were performed using Microsoft Excel. Compliance with ASTM D6751 and EN 14214 standards was then evaluated.

2.13 Statistical analysis

The study used a completely randomized design (CRD) with five light-intensity treatments (500, 2,100, 4,500, 6,000, and 8,500 lux), each combined with 15% CO_2 supplementation, and three replicates. Microsoft Excel 2016 was used to process the data, while OriginPro 2024 was used to generate the graphs. Treatment effects were analyzed by one-way ANOVA in SPSS version 25, followed by Duncan's Multiple Range Test for mean separation at $p < 0.05$.

3. Results and Discussion

3.1 Growth kinetics models

The specific growth rate of microalgae is affected by several environmental factors, including nutrients, temperature, photoperiod, and light intensity (Wahidin *et al.,* 2013). Light intensity is a critical factor affecting microalgal growth and photosynthesis, although the optimal intensity differs among species (Xu *et al.,* 2016). Because light intensity influences photosynthetic kinetics and microalgal metabolism (Difusa *et al.,* 2015), an optimal level is required for the efficient synthesis of essential molecules and cellular energy in the form of ATP and NADPH (Singh & Singh 2015).

The specific growth rate analysis demonstrated the dependence of *E. gracilis* proliferation on light intensity, with µ ranging from 0.40 day^{-1} at 500 lux to a maximum of 0.78 day^{-1} at 8,500 lux. This empirical metric was calculated directly from cell counts during the exponential phase on days 3 to 7 using Equation (2). It served as the biological reference for model validation and process optimization. Three complementary sigmoidal models (Table 1, Fig. 1) accurately described the observed growth trajectories. Each model produced the same treatment ranking: 8,500 lux > 6,000 lux > 4,500 lux > 2,100 lux > 500 lux.

The logistic model directly estimated instantaneous maximum growth rates (μ_{max} = 0.40-0.78/day) and showed strong biological agreement (R^2 = 0.88-0.96). The Gompertz model estimated relative maximum production rates (r_m = 1.20-4.95/day) and measurable lag phases (t_l = 2.83-5.29 days). These results indicated different adaptation periods across light treatments, including a lag phase of 2.83 days at 500 lux.

The Richards model provided greater mathematical resolution ($R^2 \geq 0.98$) through its flexible four-parameter structure. Its apparent maximum rates (μ_{max} = 4.61-8.77/day) exceeded the empirical µ values because the shape parameters v (18.54-192.80) and k (11.63-22.82) enabled asymmetrical curve fitting. This variation reflected treatment-specific growth dynamics, including rapid inflection at 6,000 lux (v = 192.80), rather than poor fit, as shown by the consistently high R^2 values.

Cross-model validation confirmed mathematical and biological consistency. All models produced identical treatment rankings and identified 6,000 to 8,500 lux as the optimal range. Empirical µ and logistic μ_{max} remain the primary metrics for bioprocess design, while the Gompertz and Richards models provide additional insights into lag phases and growth-trajectory complexity, respectively.

The effect of light intensity was also examined using growth kinetics modeling (Table 1 and Figure 1). Based on the logistic model, the highest maximum specific growth rate (μ_{max}) of *E. gracilis* was observed at 8,500 lux (0.78/day), while the lowest was observed at 500 lux (0.40/day). According to the Gompertz model, the highest and lowest maximum cell production rates (r_m) were also observed at 8,500 lux (4.90/day) and 500 lux (0.93/day), respectively. The Richards model produced different results, with the apparent μ_{max} reaching its fitted upper limit of 5.00/day at 4,500, 6,000, and 8,500 lux. The parameter v describes the shape and asymmetry of the fitted

Table 1
Growth kinetics model

Model	Parameters	500 Lux	2,100 Lux	4,500 Lux	6,000 Lux	8,500 Lux
Logistic model						
	μ_{max} (/day)	0.40	0.53	0.67	0.73	0.78
	R^2	0.88	0.91	0.93	0.96	0.94
Gompertz model						
	r_m (/day)	0.93	1.38	2.40	4.70	4.90
	λ	0.65	5.09	4.46	5.23	5.08
	R^2	0.84	0.91	0.91	0.94	0.93
Richards model						
	Apparent μ_{max} (/day)	2.72	3.05	5.00	5.00	5.00
	t_L	10.0	10.0	9.13	8.22	8.06
	v	5.0	5.0	5.0	2.10	1.41
	A	15.79	10.55	17.05	21.24	24.04
	R^2	0.98	0.99	0.99	0.99	0.99

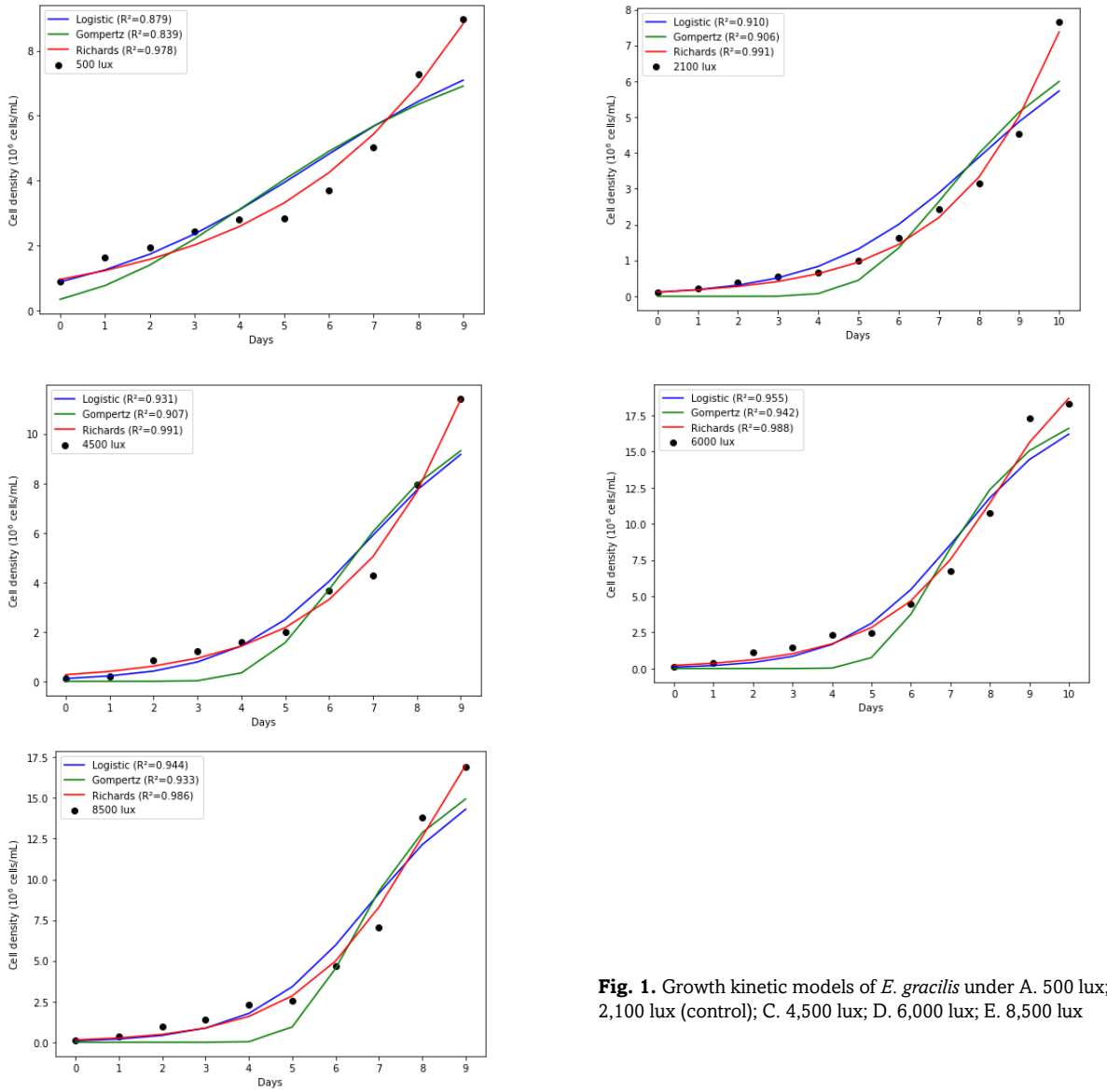

Fig. 1. Growth kinetic models of *E. gracilis* under A. 500 lux; B. 2,100 lux (control); C. 4,500 lux; D. 6,000 lux; E. 8,500 lux

curve. In this model, μ_{max} and v were fitted within preset bounds to prevent data overestimation. However, A, which represents maximum capacity, and t_l, which represents the inflection point, still differed among treatments. The model also produced high R^2 values of approximately 0.99. The three models produced R^2 values ranging from 0.84 to 0.99, indicating that they adequately described the growth of *E. gracilis*.

The Richards model complemented these analyses by providing the highest mathematical fit across all treatments ($R^2 \geq 0.98$). Its flexible four-parameter structure resulted in variation among the apparent μ_{max}, t_i, v, and A values. The decline in v from 5.00 at 500 to 4,500 lux to 1.41 at 8,500 lux reflected differences in curve shape among the light treatments. Meanwhile, A generally increased with light intensity and reached its highest value at 8,500 lux.

The parameter k (11.63-22.82) describes the steepness of the curve at the inflection point. Such variability is characteristic of flexible sigmoidal models (Lam *et al.,* 2017; Phukoetphim *et al.,* 2017) and does not indicate poor fit. Rather, it demonstrates the model's ability to capture subtle differences in growth dynamics that simpler two parameter models cannot resolve.

The biological interpretation prioritizes the logistic and Gompertz results, particularly μ_{max} and the lag phase, for process optimization. Meanwhile, the Richards model provides supplementary validation of the complexity of the growth patterns. All models consistently identified 6,000-8,500 lux as the optimal range for industrial cultivation, supporting reliable predictions of biomass productivity and process scaling.

3.2 Biomass Productivity of E. gracilis

Microalgal biomass is an essential feedstock for various biorefinery applications, including renewable fuels, bioproducts, nutraceuticals (Benedetti *et al.,* 2018), aquaculture feed ingredients, food security, and the circular economy (Ahmad *et al.,* 2022). However, microalgal biomass production is strongly affected by light intensity (Li *et al.,* 2012). Microalgae require an appropriate light intensity to achieve maximum biomass productivity (Metsoviti *et al.,* 2020).

In this study, different light intensities combined with 15% CO_2 significantly influenced the biomass productivity of *E. gracilis* ($P < 0.05$), as shown in Figure 2A. Biomass productivity increased with light intensity and peaked at 6,000 lux (0.0874 ± 0.0035 mg/mL/day), indicating the optimal light intensity under the experimental conditions. The specific growth rate of *E. gracilis* was directly related to its biomass production and productivity. However, biomass productivity decreased to 0.073 mg/mL/day at 8,500 lux. Light intensity beyond the saturation point may induce stress and reduce the final yield (Metsoviti *et al.,* 2020).

In contrast, the lowest modeled growth rate and biomass productivity were observed at 500 lux. These results indicate that *E. gracilis* requires sufficient light intensity, with 6,000 lux producing the highest biomass productivity.

Microalgae are promising feedstocks for renewable energy and high-yield green biofuels because of their primary metabolite content (Choudhary *et al.,* 2015; Zhu *et al.,* 2022). Optimizing light intensity is essential for maximizing these yields because it directly regulates photosynthetic efficiency and lipid metabolic pathways (Cheirsilp & Torpee 2012). Low light levels can inhibit growth and induce the synthesis of polar membrane lipids, whereas excessive light beyond the saturation point triggers the accumulation of neutral lipids, particularly triacylglycerols (TAGs) (Lee *et al.,* 2015; Chen *et al.,* 2017; Chen & Wang 2021). This shift is driven by increased expression of key enzymes, such as acetyl-CoA carboxylase D, which catalyzes lipid synthesis under high-light conditions (Jawaharraj *et al.,* 2016; Chen *et al.,* 2023). In addition to light, lipid productivity is influenced by the complex interactions among reactive oxygen species (ROS), nutrient availability, temperature, CO_2 levels, and genetic factors (Chen & Wang 2021; Xin *et al.,* 2024).

In addition to lipids, *E. gracilis* accumulates paramylon, a storage polysaccharide composed of β-1,3-glucan that can stimulate cytokine production (Yasuda *et al.,* 2020). To maximize lipid and paramylon yields, light duration and spectral composition must be regulated along with light intensity (Maltsev *et al.,* 2021; Wang *et al.,* 2018b). However, the optimal light intensity varies among strains.

3.3. Lipid and Paramylon Productivity of E. gracilis

According to Figure 2B-2C, differences in light intensity significantly affected lipid and paramylon productivity ($P < 0.05$). Lipid productivity increased with irradiance and reached

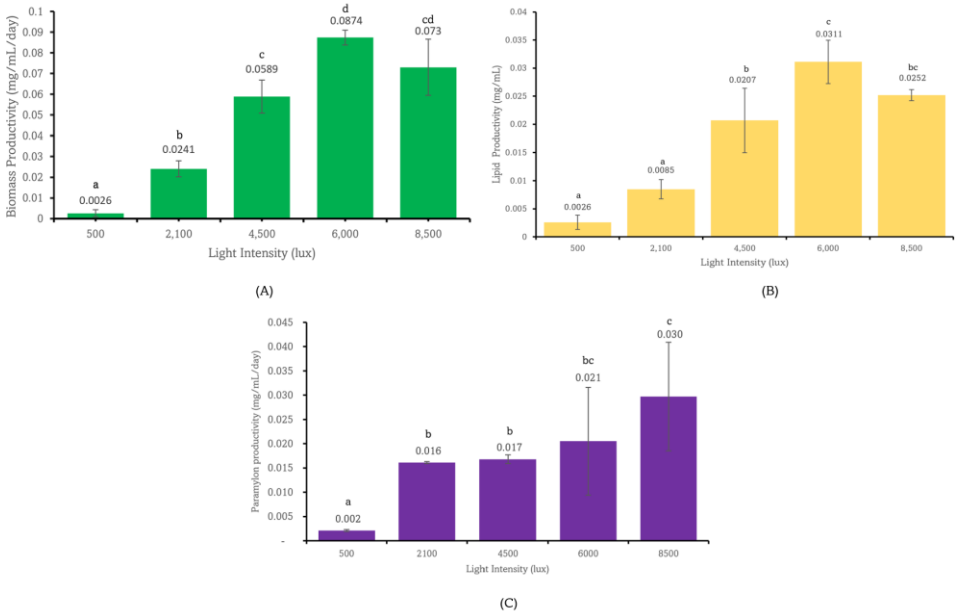

Fig. 2. Biomass productivity (A), Lipid Productivity (B), and Paramylon Productivity (C) of *E. gracilis* in different light intensity with CO_2 15%

its maximum at 6,000 lux (0.0311 ± 0.003 mg/mL/day) (Fig. 2B). However, lipid productivity decreased at 8,500 lux, although the difference from the 6,000 lux treatment was not statistically significant. This result indicates that moderate irradiance promotes carbon assimilation and fatty acid biosynthesis. It is consistent with the role of light in enhancing photosynthetic carbon fixation and activating lipid synthesis pathways in microalgae (Wang *et al.,* 2018; Maltsev *et al.,* 2021). Moderate levels of reactive oxygen species (ROS) may act as stress signals that promote lipid accumulation. However, excessive ROS levels can be toxic, inhibit TAG accumulation, and reduce photosynthetic performance (Koletti *et al.,* 2025; Miao *et al.,* 2019). Based on Figure 2C, the lowest paramylon productivity was observed at 500 lux, with a value of 0.002 ± 0.0002 mg/mL/day. This value was approximately 15 times lower than that observed at 8,500 lux. Paramylon productivity increased progressively with light intensity and reached its highest value at 8,500 lux (0.030 ± 0.0011 mg/mL/day). This result indicates that light availability influenced carbon allocation toward paramylon biosynthesis, with higher irradiance favoring paramylon accumulation. Similar findings have been reported for *Euglena gracilis*, in which paramylon accumulation is strongly influenced by culture conditions and serves as a major sink for photoassimilated carbon (Feuzing *et al.,* 2022; Muchut *et al.,* 2021; Wang *et al.,* 2018).

Increasing light intensity induced a distinct shift in carbon partitioning in the acidophilic *E. gracilis* strain. At 6,000 lux, the highest biomass and lipid productivities indicated that photosynthetic electron transport supplied sufficient ATP, NADPH, and carbon skeletons for cell growth and fatty acid synthesis. Lipid synthesis may therefore serve as a sink for excess reducing power under moderately high irradiance. At 8,500 lux, however, biomass and lipid productivity declined, while paramylon productivity continued to increase. This divergence suggests that the photosynthetic apparatus approached its saturation threshold and that newly fixed carbon was preferentially stored as paramylon rather than channeled into fatty acid synthesis (He *et al.,* 2015; Maltsev *et al.,* 2021).

Mechanistically, excess excitation energy at 8,500 lux may increase reactive oxygen species (ROS) formation and photoinhibition, as indicated by the simultaneous decreases in chlorophyll, carotenoid, biomass, and lipid productivity. Moderate ROS levels can serve as metabolic signals, whereas excessive ROS damage photosynthetic components and restrict the ATP and NADPH supply required for sustained TAG synthesis (Miao *et al.,* 2019; Lima-Melo *et al.,* 2021). Under these conditions, allocating assimilated carbon to paramylon, the principal β-1,3-glucan reserve of *E. gracilis*, may provide a readily mobilizable carbon store and reduce the metabolic burden of continued lipid synthesis. Similar paramylon accumulation under cadmium and salinity stress supports its role in cellular acclimation (He *et al.*, 2021; Kanna *et al.*, 2021). Thus, the results indicate an irradiance-dependent metabolic transition. Moderately high light favored growth and lipid production, whereas excessive light promoted photooxidative stress and carbon storage as paramylon.

3.4. Chlorophyll and Carotenoids

Microalgae use light energy to synthesize ATP and NADPH in the photosystems (Katam *et al.,* 2022). Light is absorbed primarily by chlorophyll a, the main photosynthetic pigment (Lokstein & Renger 2021). Other photosynthetic pigments also contribute to light-energy absorption. Microalgae use wavelengths of approximately 400-700 nm for photosynthesis, in green microalgae, chlorophyll a and carotenoids absorb strongly within the visible-light range (Katam *et al.,* 2022).

Consistent with Figure 3, chlorophyll a, chlorophyll b, and carotenoid contents increased with light intensity up to 6,000 lux and then declined at 8,500 lux. Chlorophyll a reached its highest value at 6,000 lux (8.31 ± 0.07 µg/mL), followed by 4,500 lux (5.95 ± 0.27 µg/mL), 8,500 lux (5.47 ± 0.15 µg/mL), 2,100 lux (3.34 ± 0.33 µg/mL), and 500 lux (0.84 ± 0.12 µg/mL). Chlorophyll b and carotenoid contents showed the same overall pattern, with the highest values at 6,000 lux and the lowest values at 500 lux. The decline at 8,500 lux is consistent with photoinhibition at excessive irradiance (González-Camejo *et al.,* 2019).

Figure 4 shows a clear irradiance-dependent shift in the pigment composition of *E. gracilis*. At 500 lux, nearly all detected pigments occurred at relatively low concentrations, indicating limited synthesis of both photosynthetic and accessory pigments under light-limited conditions. Increasing the light intensity to 2,100 lux enhanced several pigments, particularly pheophytin a, pheophytin b, β,β-carotene, and dinoxanthin, while chlorophyll c1, chlorophyll c2, violaxanthin, β-cryptoxanthin, zeaxanthin, and lutein remained comparatively low. A stronger response was observed at 4,500 lux, where pheophytin a and pheophytin b showed the greatest increases, accompanied by marked accumulation of β,β-carotene, dinoxanthin, trans- and cis-diadinoxanthin, and myxoxanthophyll. At 6,000 lux, pigment accumulation was generally maximal, pheophytin a and b remained the most abundant pigment derivatives, β,β-carotene remained high, and myxoxanthophyll, diatoxanthin, 9′-cis-neoxanthin, lutein, β-cryptoxanthin, and zeaxanthin increased relative to lower-light treatments. This broader enrichment of carotenoid and xanthophyll pigments at 6,000 lux is consistent with the maximum chlorophyll and total carotenoid contents shown in

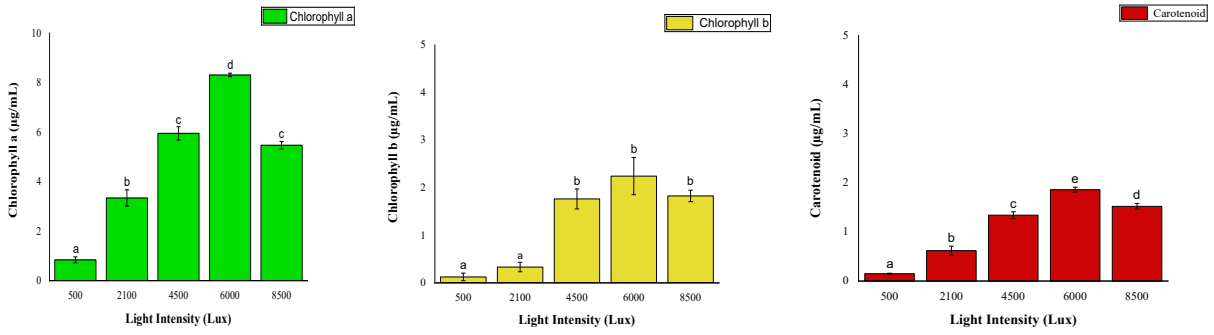

(A) (B) (C)

Fig. 3 Pigment contents of *E. gracilis*: (A) chlorophyll a, (B) chlorophyll b, and (C) carotenoids. Significant differences among light treatments are indicated by lowercase letters ($p < 0.05$, one-way ANOVA followed by Duncan's Multiple Range Test).

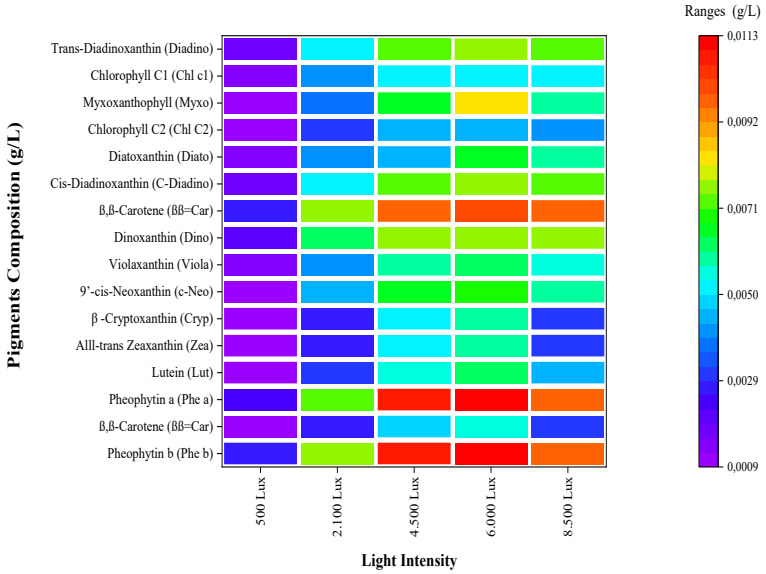

Fig 4. Pigment Composition of *E. gracilis* under different light intensities

Figure 3, suggesting enhanced light harvesting together with increased photoprotective capacity. When irradiance was further increased to 8,500 lux, pheophytin a, pheophytin b, and β,β-carotene remained dominant, whereas several accessory pigments, particularly β-cryptoxanthin, zeaxanthin, lutein, chlorophyll c1, and chlorophyll c2, declined relative to 6,000 lux. This decrease agrees with the pigment reduction observed in Figure 2 and indicates that 8,500 lux exceeded the optimal irradiance for pigment accumulation, likely promoting photoacclimation and photoinhibitory stress (Wang *et al.,* 2018; Maltsev *et al.,* 2021; Erfianti *et al.,* 2024a).

3.5. Fatty Acid Methyl Esters and Predicted Biodiesel Composition

In microalgae, TAG synthesis consists of three stages: fatty acid biosynthesis, glycerolipid formation, and lipid droplet formation (Chen & Wang 2021). Based on Table 2, light intensity altered both the diversity and relative abundance of FAMEs. The highest relative abundance of C17:1 was detected at 2,100 lux (3.81 ± 0.43), followed by 4,500 lux (3.45 ± 0.74), 6,000 lux (3.39 ± 0.98), 8,500 lux (3.13 ± 0.10), and 500 lux (2.90 ± 0.21); optimal light intensity can improve fatty acid production and quality for biodiesel applications (Nzayisenga *et al.,* 2020b), However, these differences were not statistically significant. The number of detected FAMEs was lowest at 500 lux (13 compounds), whereas the higher-light treatments showed broader profiles. This lower diversity at 500 lux coincided with the lowest biomass and lipid productivities (Fig. 2A-B). Different superscript letters within a row of Table 2 indicate statistically significant differences among light-intensity treatments ($p < 0.05$, one-way ANOVA followed by Duncan's Multiple Range Test).

Fatty acid biosynthesis in green algae occurs in the chloroplasts. During this process, pyruvate derived from glycolysis is converted into acetyl-CoA for de novo fatty acid synthesis (Zulu *et al.,* 2018). Fatty acid methyl esters (FAMEs), the main components of biodiesel, are produced through the transesterification of fats with methanol and bases such as potassium hydroxide, sodium hydroxide, or sodium methoxide (Hadiyanto *et al*, 2014; Jafarihaghighi *et al.,* 2020). FAMEs can be used as biodiesel because they reduce the corrosive effects associated with free fatty acids. Their molecular structures also influence the physical properties of the fuel and its exhaust emissions. Compared with fossil fuels, biodiesel produces lower gaseous emissions (Schobert, 2013). Moreover, FAMEs such as methyl cis-10-heptadecenoate and methyl oleate (C18:1) may be used to produce aviation biofuel. Their double bonds can be processed through catalytic cracking, hydrodeoxygenation, and other conversion methods to produce this high-value fuel.

Table 2 also shows that methyl palmitoleate (C16:1) was the predominant individual FAME across treatments. Its highest relative abundance occurred at 500 lux (32.46 ± 0.98%), but this treatment had the lowest biomass and lipid productivities (Fig. 2A-B). Thus, the high C16:1 percentage at 500 lux reflects its relative share of the FAME profile rather than the highest absolute production. At 6,000 lux, C16:1 remained abundant

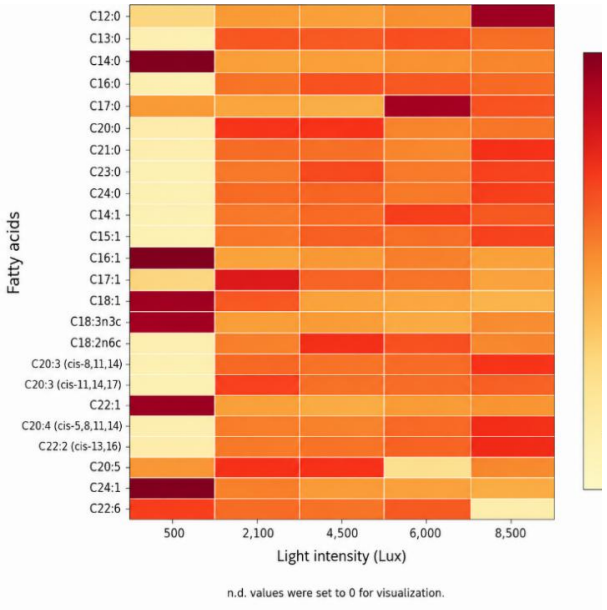

Fig. 5 Heatmap analysis of fatty acids from *E. gracilis* under different light intensities

(26.34 ± 1.68%) while biomass and lipid productivities reached their maximum, making this treatment more relevant from a production perspective. Methyl palmitate, methyl oleate, methyl stearate, and methyl linoleate are commonly reported FAME components of interest for biodiesel production (Li *et al.,* 2019).

At the fatty-acid-class level (Table 2), the highest proportions of saturated, monounsaturated, and polyunsaturated fatty acids were observed at 8,500 lux (42.35%), 500 lux (59.01%), and 4,500 lux (23.705%), respectively. Within the PUFA fraction, methyl linoleate (C18:2n6c) reached its highest relative abundance at 4,500 lux (8.71 ± 4.19), while total PUFA at 6,000 lux was slightly lower (21.32%). These results indicate that irradiance altered fatty-acid class distribution rather than causing a uniform increase or decrease across all FAMEs.

Figure 5 complements Table 2 by visualizing the relative response of individual FAMEs across the irradiance gradient using row-wise Z-score normalization. The heatmap shows that low light favored relatively high standardized values for C14:0, C16:1, C18:1, C22:1, C24:1, and C22:6, whereas C17:1 was relatively enriched at 2,100 lux and C20:0 and C18:2n6c showed stronger responses around 4,500 lux. At 6,000 lux, C17:0, C16:0, and C14:1 were comparatively high, while 8,500 lux favored several saturated and long-chain components, including C12:0, C21:0, C23:0, and C24:0. C22:6 declined markedly at the highest irradiance. Thus, Figure 5 shows that increasing light intensity remodeled the FAME profile in a compound-specific manner, consistent with irradiance-dependent fatty-acid metabolism and cellular acclimation (Constantopoulos & Bloch, 1967; Maltsev *et al*., 2021; Chen & Wang, 2021).

Table 2
Fatty acid composition of *E. gracilis* under different light intensities

Saturated	500 Lux	2,100 Lux	4,500 Lux	6,000 Lux	8,500 Lux
C12:0	n.d.	1.61±1.03^{b}	1.01±0.62^{b}	1.30±0.94^{b}	3.65±4.19^{b}
C13:0	n.d.	0.52±0.01^{b}	0.49±0.06^{b}	0.51±0.03^{b}	0.46±0.07^{b}
C14:0	14.81±0.66^{c}	5.35±0.25^{a}	5.45±0.18^{a}	6.59±0.01^{ab}	7.45±1.07^{b}
C16:0	n.d.	1.48±0.34^{b}	1.77±0.23^{b}	1.81±0.01^{b}	1.67±0.35^{b}
C17:0	3.99±0.19^{a}	3.71±0.74^{a}	3.57±0.98^{a}	5.85±0.44^{b}	4.91±0.50^{ab}
C20:0	4.99±0.11^{a}	10.99±0.11^{c}	11.13±0.45^{c}	8.55±0.57^{bc}	9.04±1.05^{b}
C21:0	4.29±0.35^{a}	11.35±0.48^{b}	10.69±1.34^{b}	10.23±2.52^{b}	13.61±1.90^{b}
C23:0	n.d.	0.67±0.01^{b}	0.82±0.07^{b}	0.67±0.18^{b}	0.86±0.11^{b}
C24:0	n.d.	0.64±0.01^{b}	0.63±0.10^{b}	0.58±0.14^{b}	0.71±0.12^{b}
Unsaturated					
C14:1	n.d.	1.84±0.42^{ab}	1.91±0.38^{ab}	2.24±1.35^{b}	1.99±0.80^{ab}
C15:1	n.d.	0.39±0.03^{b}	0.42±0.00^{b}	0.39±0.07^{b}	0.46±0.06^{b}
C16:1	32.46±0.98^{b}	24.17±1.17^{a}	25.37±1.85^{a}	26.34±1.68^{a}	24.69±0.74^{a}
C17:1	2.9±0.21^{a}	3.81±0.43^{a}	3.45±0.74^{a}	3.39±0.98^{a}	3.13±0.10^{a}
C18:1	6.98±0.47^{a}	5.74±0.13^{a}	4.28±2.14^{a}	4.34±2.27^{a}	3.95±1.39^{a}
C18:3n3c	3.05±0.57^{b}	1.63±0.06^{a}	1.59±0.30^{a}	1.52±0.40^{a}	1.76±0.26^{a}
C18:2n6c	n.d.	5.63±4.72^{a}	8.71±4.19^{a}	7.3±6.79^{a}	5.14±4.29^{a}
C20:3 (cis-8,11,14)	n.d.	1.31±0.28^{bc}	1.16±0.09^{b}	1.24±0.23^{bc}	1.63±0.11^{c}
C20:3 (cis-11,14,17)	n.d.	0.77±0.01^{c}	0.62±0.02^{bc}	0.61±0.08^{b}	0.65±0.13^{bc}
C22:1	12.41±0.06^{b}	4.27±0.28^{a}	3.66±0.04^{a}	4.44±0.40^{a}	4.33±0.78^{a}
C20:4 (cis-5,8,11,14)	3.28±0.15^{a}	4.27±0.31^{ab}	4.26±0.23^{ab}	4.44±0.62^{b}	4.75±0.57^{b}
C22:2 (cis-13,16)	n.d.	0.91±0.06^{b}	0.97±0.11^{b}	1.05±0.23^{b}	1.38±0.23^{b}
C20:5	2.61±0.16^{a}	3.48±0.09^{a}	3.45±0.32^{a}	1.73±1.75^{a}	2.61±1.65^{a}
C24:1	4.27±0.21^{b}	2.21±0.50^{a}	1.68±0.03^{a}	1.49±1.03^{a}	1.20±1.12^{a}
C22:6	3.98±0.01^{c}	3.29±0.16^{bc}	2.97±0.06^{b}	3.44±0.61^{bc}	n.d.
Saturated (%)	28.08	36.31	35.55	36.075	42.35
Monounsaturated (%)	59.01	42.415	40.745	42.605	39.76
Polyunsaturated (%)	12.91	21.275	23.705	21.32	17.9
Total (%)	100	100	100	100	100

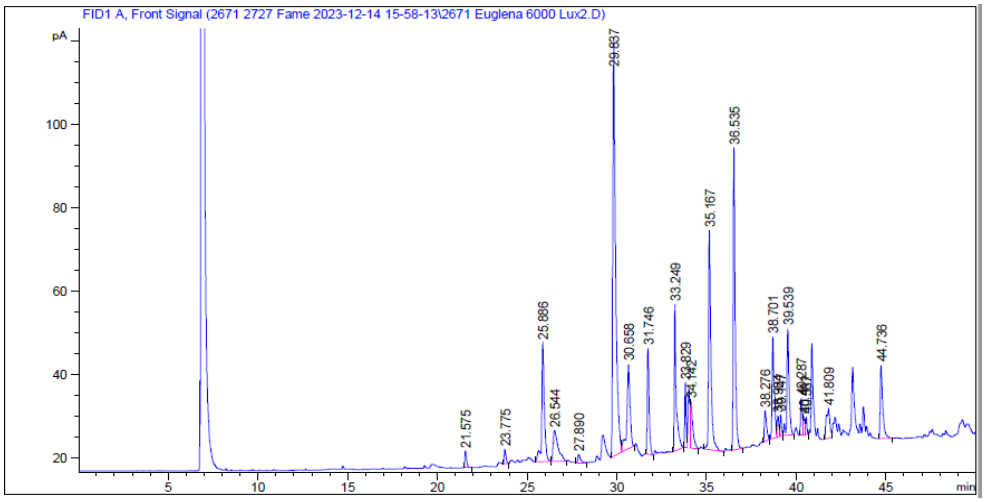

Fig. 6 Fatty acid abundance chromatogram for the 6,000 lux treatment, showing the highest peak for C16:1 FAME, methyl palmitoleate

Figure 6 provides the representative GC-FID chromatogram for the 6,000-lux treatment and shows a dominant methyl palmitoleate (C16:1) peak. The chromatograms for the other irradiance treatments are provided in Supplementary Figures S1-S4 (500, 2,100, 4,500, and 8,500 lux, respectively), while the corresponding peak areas and retention times are reported in Supplementary Tables S1-S5. Across treatments, the C16:1 peak occurred at approximately 29.78-29.84 min, supporting consistent compound assignment by comparison with the reference FAME standards. The supplementary chromatograms also corroborate the lower FAME-profile complexity at 500 lux and the broader profiles at higher irradiance. Together, Table 2, Figure 5, Figure 6, Supplementary Figures S1-S4, and Supplementary Tables S1-S5 support the conclusion that irradiance affected both the diversity and relative composition of detectable FAMEs in *E. gracilis*.

Fatty acids such as palmitic, stearic, methyl cis-10-heptadecenoate, linoleic, and linolenic acids are also relevant to biodiesel performance (Pinzi *et al.,* 2013). These light-dependent changes are biologically plausible because irradiance can modify fatty-acid synthesis and saturation patterns. High light may favor accumulation of saturated and monounsaturated fatty acids while reducing some polyunsaturated fatty acids, whereas PUFAs are particularly susceptible to oxidation because of their multiple double bonds (Maltsev *et al.,* 2021; Nzayisenga *et al.,* 2020).

The predicted biodiesel properties calculated from the GC-FID FAMEs profiles are summarized in Table 3. These values are theoretical estimates and should not be interpreted as measurements of experimentally produced biodiesel. Predicted iodine values ranged from 74.19 to 94.87 g I_2/100 g and were below the EN 14214 maximum of 120 g I_2/100 g, whereas predicted saponification values ranged from 188.53 to 192.33 mg KOH/g. Predicted cetane numbers ranged narrowly from 49.14 to 49.19, exceeding the ASTM D6751 minimum of 47 but remaining below the EN 14214 minimum of 51. The 8,500-lux treatment, which had the highest SFA fraction (Table 2), produced the lowest predicted iodine value (74.19 g I_2/100 g), whereas the more unsaturated 2,100-4,500-lux treatments had higher iodine values. At 6,000 lux, the highest measured lipid productivity (Fig. 2B) was accompanied by intermediate predicted values (IV 89.67 g I_2/100 g; SV 190.99 mg KOH/g; CN 49.16), supporting its selection for subsequent biodiesel validation.

Accordingly, Table 3 provides a feedstock-level prediction rather than direct evidence of finished-biodiesel performance. Future studies should convert the extracted lipids into biodiesel and directly measure cetane number, oxidative stability, viscosity, density, acid value, and cold-flow properties using standardized methods before claims of compliance with ASTM D6751 or EN 14214 are made.

Three key characteristics of biodiesel are cetane number, cloud point, and oxidative stability. The cetane number indicates the ignition quality of biodiesel in diesel engines. A higher cetane number generally indicates better ignition performance. The cloud point indicates the temperature at which wax crystals begin to form and affect fuel fluidity. Therefore, a lower cloud point is preferable for use at low temperatures. Oxidative stability indicates the fuel's resistance to degradation during storage, with greater stability reflecting better storage performance (Liu & Renock, 2021). Other important biodiesel characteristics include heat of combustion, viscosity, and lubricity, which refers to the fuel's ability to lubricate engine components (Knothe, 2005).

Table 3
Predicted Biodiesel Properties Based on Average FAME Profiles

Light intensity	Iodine value (IV), g I_2/100 g	Saponification value (SV)	Cetane number (CN)
500 Lux	91.81	192.33	49.14
2100 Lux	92.96	188.53	49.19
4500 Lux	94.87	189.12	49.18
6000 Lux	89.67	190.99	49.16
8500 Lux	74.19	192.03	49.14

In addition to having a high lipid content, microalgal lipids should meet biodiesel standards and contain favorable fatty acid profiles. Lipids with higher levels of unsaturated fatty acids are more susceptible to oxidation. Therefore, suitable biodiesel feedstocks generally contain more monounsaturated fatty acids than saturated fatty acids, which are prone to solidification, and polyunsaturated fatty acids, which are prone to oxidation (Sharmin *et al.,* 2016).

The proportions of monounsaturated fatty acids (MUFAs), saturated fatty acids (SFAs), and polyunsaturated fatty acids (PUFAs) determine biodiesel characteristics. SFAs are straight-chain hydrocarbons with a carboxyl group, whereas MUFAs and PUFAs contain one or more double bonds. Lipids rich in SFAs, such as C12:0, C14:0, C18:0, C20:0, and C22:0, generally have higher cetane numbers, cloud points, and oxidative stability. Although such biodiesel has favorable ignition quality and oxidative stability, its high cloud point may reduce fluidity at low temperatures. Biodiesel rich in MUFAs, such as C16:1, C18:1, C20:1, and C22:1, generally offers a better balance of properties than biodiesel dominated by SFAs or PUFAs. It typically has intermediate cetane numbers, cloud points, and oxidative stability. In contrast, biodiesel dominated by PUFAs, such as C18:2, C18:3, C20:4, and C20:5, generally has lower cetane numbers, cloud points, and oxidative stability. Although the lower cloud point improves low-temperature fluidity, poor ignition quality and oxidative stability may limit biodiesel performance (Liu & Renock, 2021).

Across all treatments, MUFAs remained the dominant fatty-acid class (39.76-59.01% of total FAMEs; Table 2). This composition is potentially favorable because MUFAs can provide a balance between the oxidative stability associated with SFAs and the improved low-temperature fluidity associated with PUFAs. Nevertheless, biodiesel quality depends on chain length, degree and position of unsaturation, minor compounds, and the overall SFA-MUFA-PUFA balance; therefore, the composition remains subject to direct fuel-property testing (Knothe, 2005; Anwar *et al.,* 2018; Mekonnen *et al.*, 2024). When production performance and composition are considered together, the 6,000-lux treatment provides the strongest overall candidate for further biodiesel evaluation: it produced the highest lipid productivity (Fig. 2B), retained a MUFA-dominated FAME profile (Table 2), and showed intermediate predicted IV, SV, and CN values (Table 3). This interpretation is based on the combined productivity-profile balance rather than on the maximum relative abundance of a single FAME.

A previous study successfully characterized *euglena*-based biodiesel. The saponification number (SN) ranged from 208.1 to 227.1, below the maximum value of 370 specified by ASTM D6751 (Chen *et al.,* 2022; Sakthivel *et al.,* 2018). The iodine number (IN) ranged from 56.6 to 200, while the stated standard value was 125. The cetane number (CN) ranged from 27.6 to 57.6, compared with an international minimum standard of 45. Although the MUFA content was lower than the PUFA and SFA contents, some of the predicted biodiesel properties remained within the reported acceptable ranges (Chen *et al.,* 2022).

Overall, the substantial C16-C18 FAME fractions, particularly methyl palmitoleate, support the potential use of this biomass as a biodiesel feedstock. The calculated iodine, saponification, and cetane values provide preliminary indications of expected fuel behavior. However, these values remain predictions based on fatty acid composition. Because biodiesel conversion and standardized fuel testing were not conducted, the findings should be interpreted as a feedstock screening assessment rather than confirmation of commercial biodiesel quality.

4. Conclusion

Light intensity significantly affected biomass formation, carbon partitioning, pigment accumulation, and FAME composition in the acidophilic *E. gracilis* strain cultivated with 15% CO_2. The optimal treatment for biomass and lipid production was 6,000 lux, which yielded biomass and lipid productivities of 0.0874 ± 0.0035 and 0.0311 ± 0.0030 mg mL^{-1} day^{-1}, respectively. Increasing the irradiance to 8,500 lux reduced biomass and lipid productivity but produced the highest paramylon productivity (0.030 ± 0.0011 mg mL^{-1} day^{-1}). This result indicated a shift in assimilated carbon allocation from lipid synthesis to paramylon storage. Methyl palmitoleate (C16:1) was the predominant individual FAME. At 6,000 lux, the FAME profile comprised 42.61% MUFAs, 36.08% SFAs, and 21.32% PUFAs. The predicted iodine value, saponification value, and cetane number were 89.67 g I_2/100 g, 190.99 mg KOH/g, and 49.16, respectively. These predicted properties indicate promising feedstock characteristics but cannot replace biodiesel conversion and standardized fuel testing. Thus, 6,000 lux provided the best balance among measured biomass productivity, lipid productivity, and theoretically estimated biodiesel feedstock quality, whereas 8,500 lux favored paramylon accumulation.

Acknowledgements

This manuscript is part of a thesis. The authors thank the Laboratory of Biotechnology, Faculty of Biology, Universitas Gadjah Mada, for providing research facilities and support.

Supplementary information

Supllementrary information of this article can be accessed: https://ijred.cbiore.id/index.php/ijred/article/downloadSuppFile/61637/16610

Author Contribution: Aritonang, D.: conceptualization, methodology, formal analysis, and writing, original draft; Erfianti, T.: writing, review and editing, project administration, and validation; Putri, R.A.E.: writing, review and editing, project administration, and validation; Kartina: writing, review and editing, project administration, and validation; Ramadhana, S.D.: writing, review and editing, project administration, and validation; Sadewo, B.R.: software, validation, and writing, review and editing. Asiandu, A.P.: writing, review and editing, project administration, and validation; Suyono, E.A.: supervision, resources, and project administration; All authors have read and approved the final version of the manuscript.

Funding: This research was funded by Universitas Gadjah Mada through the 2024 RTA (Rekognisi Tugas Akhir) program under contract number 370/UN.P1/KPT/HUKOR/2024.

Conflicts of Interest: The authors declare no conflicts of interest.

References

Ahmad, A., Hassan, S. W., & Banat, F. (2022). An overview of microalgae biomass as a sustainable aquaculture feed ingredient: Food security and circular economy. *Bioengineered, 13*(4), 9521-9547. https://doi.org/10.1080/21655979.2022.2061148

Anwar, M., Rasul, M. G., Ashwath, N., & Rahman, M. M. (2018). Optimisation of second-generation biodiesel production from Australian native stone fruit oil using response surface method. *Energies, 11*(10), 2566. https://doi.org/10.3390/en11102566

ASTM International. (2023). *Standard specification for biodiesel fuel blend stock (B100) for middle distillate fuels (ASTM D6751-23).* https://doi.org/10.1520/D6751-23

Barsanti, L., Vismara, R., Passarelli, V., & Gualtieri, P. (2001). Paramylon (beta-1,3-glucan) content in wild type and WZSL mutant of *Euglena gracilis*: Effects of growth conditions. *Journal of Applied Phycology, 13*(1), 59-65. https://doi.org/10.1023/A:1008105416065

Benedetti, M., Vecchi, V., Barera, S., & Dall'Osto, L. (2018). Biomass from microalgae: The potential of domestication towards sustainable biofactories. *Microbial Cell Factories, 17*, 173. https://doi.org/10.1186/s12934-018-1019-3

Bligh, E. G., & Dyer, W. J. (1959). A rapid method of total lipid extraction and purification. *Canadian Journal of Biochemistry and Physiology, 37*(8), 911-917. https://doi.org/10.1139/o59-099

Bogue, J. P., Smith, L. F., & Lipsett, L. (1957). A practical handbook. *The Journal of Higher Education, 28*(7), 405.

Carvalho, A. P., Silva, S. O., Baptista, J. M., & Malcata, F. X. (2011). Light requirements in microalgal photobioreactors: An overview of biophotonic aspects. *Applied Microbiology and Biotechnology, 89*(5), 1275-1288. https://doi.org/10.1007/s00253-010-3047-8

Cheirsilp, B., & Torpee, S. (2012). Enhanced growth and lipid production of microalgae under mixotrophic culture condition: Effect of light intensity, glucose concentration and fed-batch cultivation. *Bioresource Technology, 110*, 510-516. https://doi.org/10.1016/j.biortech.2012.01.125

Chen, B., Wan, C., Mehmood, M. A., Chang, J.-S., Bai, F., & Zhao, X. (2017). Manipulating environmental stresses and stress tolerance of microalgae for enhanced production of lipids and value-added products: A review. *Bioresource Technology, 244*, 1198-1206. https://doi.org/10.1016/j.biortech.2017.05.170

Chen, H., & Wang, Q. (2021). Regulatory mechanisms of lipid biosynthesis in microalgae. *Biological Reviews, 96*(5), 2373-2391. https://doi.org/10.1111/brv.12759

Chen, S., Li, X., Ma, X., Qing, R., Chen, Y., Zhou, H., Yu, Y., Li, J., & Tan, Z. (2023). Lighting the way to sustainable development: Physiological response and light control strategy in microalgae-based wastewater treatment under illumination. *Science of the Total Environment, 903*, 166298. https://doi.org/10.1016/j.scitotenv.2023.166298

Chen, Z., Chen, Y., Zhang, H., Qin, H., He, J., Zheng, Z., Zhao, L., Lei, A., & Wang, J. (2022). Evaluation of *Euglena gracilis* 815 as a new candidate for biodiesel production. *Frontiers in Bioengineering and Biotechnology, 10*, 827513. https://doi.org/10.3389/fbioe.2022.827513

Choudhary, P., Bhattacharya, A., Prajapati, S. K., Kaushik, P., & Malik, A. (2015). Phycoremediation-coupled biomethanation of microalgal biomass. In S.-K. Kim (Ed.), *Handbook of marine microalgae: Biotechnology advances* (pp. 483-499). Elsevier. https://doi.org/10.1016/B978-0-12-800776-1.00032-7

Constantopoulos, G., & Bloch, K. (1967). Effect of light intensity on the lipid composition of *Euglena gracilis*. *Journal of Biological Chemistry, 242*(15), 3538-3542. https://doi.org/10.1016/S0021-9258(18)95895-3

Cramer, M., & Myers, J. (1952). Growth and photosynthetic characteristics of *Euglena gracilis*. *Archiv fur Mikrobiologie, 17*, 384-402. https://doi.org/10.1007/BF00410835

Difusa, A., Talukdar, J., Kalita, M. C., Mohanty, K., & Goud, V. V. (2015). Effect of light intensity and pH condition on the growth, biomass and lipid content of microalgae *Scenedesmus* species. *Biofuels, 6*(1-2), 37-44. https://doi.org/10.1080/17597269.2015.1045274

Dubois, M., Gilles, K., Hamilton, J. K., Rebers, P. A., & Smith, F. (1951). A colorimetric method for the determination of sugars. *Nature, 168*, 167. https://doi.org/10.1038/168167a0

Erfianti, T., Daryono, B. S., Budiman, A., & Suyono, E. A. (2024c). Growth and metabolite enhancement of acidophile *Euglena* sp. isolated from Indonesia under different photoperiod cycles. *Jurnal Ilmiah Perikanan dan Kelautan, 16*(1), 130-150. https://doi.org/10.20473/jipk.v16i1.46193

Erfianti, T., Sadewo, B. R., Daryono, B. S., Budiman, A., & Suyono, E. A. (2024b). Evaluating CO_2 concentration effects on growth kinetics and fatty acid composition in *Euglena gracilis*. *Applied Phycology, 5*(1), 61-71. https://doi.org/10.1080/26388081.2024.2382866

Erfianti, T., Yusuf, A. F., Handayani, S., Sadewo, B. R., Daryono, B. S., Budiman, A., & Suyono, E. A. (2024a). Enhancing growth and metabolite profiles in indigenous *Euglena gracilis* through explorative light spectrum effect. *The Egyptian Journal of Aquatic Research, 50*(3), 318-331. https://doi.org/10.1016/j.ejar.2024.09.003

European Committee for Standardization. (2012). *Liquid petroleum products - Fatty acid methyl esters (FAME) for use in diesel engines and heating applications - Requirements and test methods (EN 14214:2012).*

Feuzing, F., Mbakidi, J.-P., Marchal, L., Bouquillon, S., & Leroy, E. (2022). A review of paramylon processing routes from microalga biomass to non-derivatized and chemically modified products. *Carbohydrate Polymers, 288*, 119181. https://doi.org/10.1016/j.carbpol.2022.119181

Friedlingstein, P., O'Sullivan, M., Jones, M. W., Andrew, R. M., Gregor, L., Hauck, J., Le Quere, C., Luijkx, I. T., Olsen, A., Peters, G. P., Peters, W., Pongratz, J., Schwingshackl, C., Sitch, S., Canadell, J. G., Ciais, P., Jackson, R. B., Alin, S. R., Alkama, R., ... Zheng, B. (2022). Global Carbon Budget 2022. *Earth System Science Data, 14*, 4811-4900. https://doi.org/10.5194/essd-14-4811-2022

Gissibl, A., Sun, A., Care, A., Nevalainen, H., & Sunna, A. (2019). Bioproducts from *Euglena gracilis*: Synthesis and applications. *Frontiers in Bioengineering and Biotechnology, 7*, 108. https://doi.org/10.3389/fbioe.2019.00108

Gonzalez-Camejo, J., Viruela, A., Ruano, M. V., Barat, R., Seco, A., & Ferrer, J. (2019). Effect of light intensity, light duration and photoperiods in the performance of an outdoor photobioreactor for urban wastewater treatment. *Algal Research, 40*, 101511. https://doi.org/10.1016/j.algal.2019.101511

Gopinath, A., Puhan, S., & Nagarajan, G. (2009). Theoretical modeling of iodine value and saponification value of biodiesel fuels from their fatty acid composition. *Renewable Energy, 34*(7), 1806-1811. https://doi.org/10.1016/j.renene.2008.11.023

Hadiyanto, H.,Nur, M.M.A. (2014). Lipid extraction of microalga Chlorella sp. cultivated in palm oil mill effluent (POME) medium. *World Applied Sciences Journal*, 31(5), 959–967. https://doi.org/10.5829/idosi.wasj.2014.31.05.2006

Hanief, S., Prasakti, L., Pradana, Y. S., Cahyono, R. B., & Budiman, A. (2020). Growth kinetic of *Botryococcus braunii* microalgae using logistic and Gompertz models. *AIP Conference Proceedings, 2296*(1), 020065. https://doi.org/10.1063/5.0030459

He, J., Liu, C. C., Du, M., Zhou, X., Hu, Z., Lei, A., & Wang, J. (2021). Metabolic responses of a model green microalga *Euglena gracilis* to different environmental stresses. *Frontiers in Bioengineering and Biotechnology, 9*, 662655. https://doi.org/10.3389/fbioe.2021.662655

He, Q., Yang, H., Wu, L., & Hu, C. (2015). Effect of light intensity on physiological changes, carbon allocation and neutral lipid accumulation in oleaginous microalgae. *Bioresource Technology, 191*, 219-228. https://doi.org/10.1016/j.biortech.2015.05.021

Herzog, H., Eliasson, B., & Kaarstad, O. (2000). Capturing greenhouse gases. *Scientific American, 282*(2), 72-79. https://doi.org/10.1038/scientificamerican0200-72

Husna, F., Rachmawati, B., Samudra, T. T., Pradana, Y. S., Budiman, A., & Suyono, E. A. (2020). Effectivity of various media for biomass and lipid production of mixed culture of Glagah in open pond. *AIP Conference Proceedings, 2260*(1), 040017. https://doi.org/10.1063/5.0016181

Ievina, B., & Romagnoli, F. (2020). Effect of light intensity on the growth of three microalgae in laboratory batch cultures. *Proceedings of the 28th European Biomass Conference and Exhibition*, 169-175. https://doi.org/10.5071/28thEUBCE2020-1DV.1.26

Indahsari, H. S., Tassakka, A. C. M. A. R., Dewi, E. N., Yuwono, M., & Suyono, E. A. (2022). Effects of salinity and bioflocculation during *Euglena* sp. harvest on the production of lipid, chlorophyll, and carotenoid with *Skeletonema* sp. as a bioflocculant. *Journal of Pure and Applied Microbiology, 16*(4), 2901-2911. https://doi.org/10.22207/JPAM.16.4.65

Jafarihaghighi, F., Ardjmand, M., Salar Hassani, M., Mirzajanzadeh, M., & Bahrami, H. (2020). Effect of fatty acid profiles and molecular structures of nine new sources of biodiesel on combustion and emission. *ACS Omega, 5*(26), 16053-16063. https://doi.org/10.1021/acsomega.0c01526

Jawaharraj, K., Karpagam, R., Ashokkumar, B., Pratheeba, C. N., & Varalakshmi, P. (2016). Enhancement of biodiesel potential in cyanobacteria: Using agro-industrial wastes for fuel production, properties and acetyl-CoA carboxylase D (accD) gene expression of *Synechocystis* sp. *Renewable Energy, 98*, 72-77. https://doi.org/10.1016/j.renene.2016.02.038

Kanna, S. D., Domonkos, I., Kobori, T. O., Dergez, A., Bode, K., Nagyapati, S., Zsiros, O., Unnep, R., Nagy, G., Garab, G., Szilak, L., Solymosi, K., Kovacs, L., & Ughy, B. (2021). Salt stress induces paramylon accumulation and fine-tuning of the macro-organization of thylakoid membranes in *Euglena gracilis* cells. *Frontiers in Plant Science, 12*, 725699. https://doi.org/10.3389/fpls.2021.725699

Katam, K., Ananthula, R., Anumala, S., Sriariyanun, M., & Bhattacharyya, D. (2022). The impact of light intensity and wavelength on the performance of algal-bacterial culture treating domestic wastewater. *E3S Web of Conferences, 355*, 02003. https://doi.org/10.1051/e3sconf/202235502003

Kitaya, Y., Azuma, H., & Kiyota, M. (2005). Effects of temperature, CO_2/O_2 concentrations and light intensity on cellular multiplication of microalgae, *Euglena gracilis*. *Advances in Space Research, 35*(9), 1584-1588. https://doi.org/10.1016/j.asr.2005.03.039

Klopfenstein, W. E. (1985). Effect of molecular weights of fatty acid esters on cetane numbers as diesel fuels. *Journal of the American Oil Chemists' Society, 62*(6), 1029-1031. https://doi.org/10.1007/BF02935708

Knothe, G. (2005). Dependence of biodiesel fuel properties on the structure of fatty acid alkyl esters. *Fuel Processing Technology, 86*(10), 1059-1070. https://doi.org/10.1016/j.fuproc.2004.11.002

Koletti, A., Skliros, D., Dervisi, I., Roussis, A., & Flemetakis, E. (2025). Oxidative stress responses in microalgae: Modern insights into an old topic. *Applied Microbiology, 5*(2), 37. https://doi.org/10.3390/applmicrobiol5020037

Krichen, E., Rapaport, A., Le Floc'h, E., & Fouilland, E. (2021). A new kinetics model to predict the growth of micro-algae subjected to fluctuating availability of light. *Algal Research, 58*, 102362. https://doi.org/10.1016/j.algal.2021.102362

Lam, M. K., Yusoff, M. I., Uemura, Y., Lim, J. W., Khoo, C. G., Lee, K. T., & Ong, H. C. (2017). Cultivation of *Chlorella vulgaris* using nutrients source from domestic wastewater for biodiesel production: Growth condition and kinetic studies. *Renewable Energy, 103*, 197-207. https://doi.org/10.1016/j.renene.2016.11.032

Lee, E., Jalalizadeh, M., & Zhang, Q. (2015). Growth kinetic models for microalgae cultivation: A review. *Algal Research, 12*, 497-512. https://doi.org/10.1016/j.algal.2015.10.004

Lenka, S. K., Carbonaro, N., Park, R., Miller, S. M., Thorpe, I., & Li, Y. (2016). Current advances in molecular, biochemical, and computational modeling analysis of microalgal triacylglycerol biosynthesis. *Biotechnology Advances, 34*(5), 1046-1063. https://doi.org/10.1016/j.biotechadv.2016.06.004

Li, F., Liu, Z., Ni, Z., & Wang, H. (2019). Effect of biodiesel components on its lubrication performance. *Journal of Materials Research and Technology, 8*(5), 3681-3687. https://doi.org/10.1016/j.jmrt.2019.06.011

Li, Y., Zhou, W., Hu, B., Min, M., Chen, P., & Ruan, R. R. (2012). Effect of light intensity on algal biomass accumulation and biodiesel production for mixotrophic strains *Chlorella kessleri* and *Chlorella protothecoides* cultivated in highly concentrated municipal wastewater. *Biotechnology and Bioengineering, 109*(9), 2222-2229. https://doi.org/10.1002/bit.24491

Lima-Melo, Y., Kilic, M., Aro, E.-M., & Gollan, P. J. (2021). Photosystem I inhibition, protection and signalling: Knowns and unknowns. *Frontiers in Plant Science, 12*, 791124. https://doi.org/10.3389/fpls.2021.791124

Liu, S. D., & Renock, D. (2021). Optimizing *Nannochloropsis* growing conditions for biodiesel production through analysis of lipid content. *ChemRxiv*. https://doi.org/10.26434/chemrxiv.14551329.v1

Lokstein, H., Renger, G., & Gotze, J. P. (2021). Photosynthetic light-harvesting (antenna) complexes-structures and functions. *Molecules, 26*(11), 3378. https://doi.org/10.3390/molecules26113378

Maltsev, Y., Maltseva, K., Kulikovskiy, M., & Maltseva, S. (2021). Influence of light conditions on microalgae growth and content of lipids, carotenoids, and fatty acid composition. *Biology, 10*(10), 1060. https://doi.org/10.3390/biology10101060

Mekonnen, K. D., Endris, Y. A., & Abdu, K. Y. (2024). Alternative methods for biodiesel cetane number valuation: A technical note. *ACS Omega, 9*(6), 6277-6284. https://doi.org/10.1021/acsomega.3c09216

Metsoviti, M. N., Papapolymerou, G., Karapanagiotidis, I. T., & Katsoulas, N. (2019). Comparison of growth rate and nutrient content of five microalgae species cultivated in greenhouses. *Plants, 8*(8), 279. https://doi.org/10.3390/plants8080279

Metsoviti, M. N., Papapolymerou, G., Karapanagiotidis, I. T., & Katsoulas, N. (2020). Effect of light intensity and quality on growth rate and composition of *Chlorella vulgaris*. *Plants, 9*(1), 31. https://doi.org/10.3390/plants9010031

Miao, R., Ma, X., Deng, X., & Huang, K. (2019). High level of reactive oxygen species inhibits triacylglycerols accumulation in *Chlamydomonas reinhardtii*. *Algal Research, 38*, 101400. https://doi.org/10.1016/j.algal.2018.101400

Muchut, R. J., Calloni, R. D., Arias, D. G., Guerrero, S. A., Iglesias, A. A., & Poklepovich, T. J. (2021). Elucidating carbohydrate metabolism in *Euglena gracilis*: Reverse genetics-based evaluation of genes coding for enzymes linked to paramylon accumulation. *Biochimie, 184*, 125-131. https://doi.org/10.1016/j.biochi.2021.02.016

Nur, F., Erfianti, T., Andeska, D. P., Putri, R. A. E., Nurafifah, I., Sadewo, B. R., & Suyono, E. A. (2023). Enhancement of microalgal metabolite production through *Euglena* sp. local strain and Glagah strain consortia. *Biosaintifika: Journal of Biology & Biology Education, 15*(1), 36-47. https://doi.org/10.15294/biosaintifika.v15i1.41895

Nurafifah, I., Hardianto, M. A., Erfianti, T., Amelia, R., Maghfiroh, K. Q., Kurnianto, D., Siswanti, D. U., Sadewo, B. R., Putri, R. A. E., & Suyono, E. A. (2023). The effect of acidic pH on growth kinetics, biomass productivity, and primary metabolite contents of *Euglena* sp. *Makara Journal of Science, 27*(2), 97-105. https://doi.org/10.7454/mss.v27i2.1506

Nzayisenga, J. C., Farge, X., Groll, S. L., & Sellstedt, A. (2020). Effects of light intensity on growth and lipid production in microalgae grown in wastewater. *Biotechnology for Biofuels, 13*, 4. https://doi.org/10.1186/s13068-019-1646-x

Olguin, E. J., Dorantes, E., Castillo, O. S., & Hernandez-Landa, V. J. (2015). Anaerobic digestates from vinasse promote growth and lipid enrichment in *Neochloris oleoabundans* cultures. *Journal of Applied Phycology, 27*(5), 1813-1822. https://doi.org/10.1007/s10811-015-0540-6

Onyeaka, H., Miri, T., Obileke, K. C., Hart, A., Anumudu, C., & Al-Sharify, Z. T. (2021). Minimizing carbon footprint via microalgae as a biological capture. *Carbon Capture Science & Technology, 1*, 100007. https://doi.org/10.1016/j.ccst.2021.100007

Ozasa, K., Won, J., Song, S., Shinomura, T., & Maeda, M. (2019). Phototaxis and photo-shock responses of *Euglena gracilis* under gravitaxis. *Algal Research, 41*, 101563. https://doi.org/10.1016/j.algal.2019.101563

Papilo, P., Marimin, Hambali, E., Machfud, Yani, M., Asrol, M., Evanila, Prasetya, H., & Mahmud, J. (2022). Palm oil-based bioenergy sustainability and policy in Indonesia and Malaysia: A systematic review and future agendas. *Heliyon, 8*(10), e10919. https://doi.org/10.1016/j.heliyon.2022.e10919

Phukoetphim, N., Salakkam, A., Laopaiboon, P., & Laopaiboon, L. (2017). Kinetic models for batch ethanol production from sweet sorghum juice under normal and high gravity fermentations: Logistic and modified Gompertz models. *Journal of Biotechnology, 243*, 69-75. https://doi.org/10.1016/j.jbiotec.2016.12.012

Pinzi, S., Rounce, P., Herreros, J. M., Tsolakis, A., & Dorado, M. P. (2013). The effect of biodiesel fatty acid composition on combustion and diesel engine exhaust emissions. *Fuel, 104*, 170-182. https://doi.org/10.1016/j.fuel.2012.08.056

Praharyawan, S., Rahman, D. Y., & Susilaningsih, D. (2016). Characterization of lipid productivity and fatty acid profile of three fast-growing microalgae isolated from Bengkulu for possible use in health application. *Journal of Tropical Life Science, 6*(2), 79-85. https://doi.org/10.11594/jtls.06.02.03

Pruvost, J., Van Vooren, G., Le Gouic, B., Couzinet-Mossion, A., & Legrand, J. (2011). Systematic investigation of biomass and lipid productivity by microalgae in photobioreactors for biodiesel application. *Bioresource Technology, 102*(1), 150-158. https://doi.org/10.1016/j.biortech.2010.06.153

Ramadhana, S. D., Erfianti, T., Aritonang, D., & Suyono, E. A. (2025). Influence of nitrogen variation and 15% CO_2 injection on wax ester production in *Euglena gracilis* isolated from Dieng Peatland, Indonesia. *Applied Phycology, 6*(1), 190-209. https://doi.org/10.1080/26388081.2025.2509212

Ritchie, R. J. (2006). Consistent sets of spectrophotometric chlorophyll equations for acetone, methanol and ethanol solvents. *Photosynthesis Research, 89*(1), 27-41. https://doi.org/10.1007/s11120-006-9065-9

Sakthivel, R., Ramesh, K., Purnachandran, R., & Mohamed, S. P. (2018). A review on the properties, performance and emission aspects of the third generation biodiesels. *Renewable and Sustainable Energy Reviews, 82*, 2970-2992. https://doi.org/10.1016/j.rser.2017.10.037

Sathya, A. B., Thirunavukkarasu, A., Nithya, R., Nandan, A., Sakthishobana, K., Kola, A. K., Sivashankar, R., Tuan, H. A., & Deepanraj, B. (2023). Microalgal biofuel production: Potential challenges and prospective research. *Fuel, 332*, 126199. https://doi.org/10.1016/j.fuel.2022.126199

Schobert, H. H. (2013). *Chemistry of fossil fuels and biofuels*. Cambridge University Press. https://doi.org/10.1017/CBO9780511844188

Sharmin, T., Hasan, C. M., Aftabuddin, S., Rahman, A., & Khan, M. (2016). Growth, fatty acid, and lipid composition of marine microalgae *Skeletonema costatum* available in Bangladesh coast: Consideration as biodiesel feedstock. *Journal of Marine Biology, 2016*, 6832847. https://doi.org/10.1155/2016/6832847

Shokravi, H., Heidarrezaei, M., Shokravi, Z., Ong, H. C., Lau, W. J., Md Din, M. F., & Ismail, A. F. (2022). Fourth generation biofuel from genetically modified algal biomass for bioeconomic development. *Journal of Biotechnology, 360*, 23-36. https://doi.org/10.1016/j.jbiotec.2022.10.010

Singh, R., Langyan, S., Rohtagi, B., Darjee, S., & Khandelwal, A. (2022). Production of biofuels options by contribution of effective and suitable enzymes: Technological developments and challenges. *Materials Science for Energy Technologies, 5*, 294-310. https://doi.org/10.1016/j.mset.2022.05.001

Singh, S. P., & Singh, P. (2015). Effect of temperature and light on the growth of algae species: A review. *Renewable and Sustainable Energy Reviews, 50*, 431-444. https://doi.org/10.1016/j.rser.2015.05.024

Solovchenko, A. E. (2012). Physiological role of neutral lipid accumulation in eukaryotic microalgae under stresses. *Russian Journal of Plant Physiology, 59*(2), 167-176. https://doi.org/10.1134/S1021443712020161

Song, X., Liu, B., Kong, F., Song, Q., Ren, N., & Ren, H. (2023). Lipid accumulation by a novel microalga *Parachlorella kessleri* R-3 with wide pH tolerance for promising biodiesel production. *Algal Research, 69*, 102925. https://doi.org/10.1016/j.algal.2022.102925

Suzuki, K. (2017). Large-scale cultivation of *Euglena*. In S. D. Schwartzbach & S. Shigeoka (Eds.), *Euglena: Biochemistry, cell and molecular biology* (pp. 285-293). Springer. https://doi.org/10.1007/978-3-319-54910-1_14

Thrane, J.-E., Kyle, M., Striebel, M., Haande, S., Grung, M., Rohrlack, T., & Andersen, T. (2015). Spectrophotometric analysis of pigments: A critical assessment of a high-throughput method for analysis of algal pigment mixtures by spectral deconvolution. *PLOS ONE, 10*(9), e0137645. https://doi.org/10.1371/journal.pone.0137645

Uliesther, N., Nurafifah, I., Rohmawati, I., Putri, R. A. E., Erfianti, T., & Suyono, E. A. (2023). Different carbon source alternative medium improves *Euglena* sp. growth and paramylon production. *Biogenesis: Jurnal Ilmiah Biologi, 11*(1), 102-113. https://doi.org/10.24252/bio.v11i1.35221

Wahidin, S., Idris, A., & Shaleh, S. R. M. (2013). The influence of light intensity and photoperiod on the growth and lipid content of microalgae *Nannochloropsis* sp. *Bioresource Technology, 129*, 7-11. https://doi.org/10.1016/j.biortech.2012.11.032

Wang, Y., Seppanen-Laakso, T., Rischer, H., & Wiebe, M. G. (2018). *Euglena gracilis* growth and cell composition under different temperature, light and trophic conditions. *PLOS ONE, 13*(4), e0195329. https://doi.org/10.1371/journal.pone.0195329

Wardana, W. E., Tantri, D. H., Afifah, M. N. R., Aini, H. N., Siswanti, D. U., Maghfiroh, K. Q., Erfianti, T., Amelia, R., Kurnianto, D., & Suyono, E. A. (2023). Effect of mercury stress on the growth and lipid content of *Euglena* sp. and *Echinodorus palaefolius*. *Jurnal Biodjati, 8*(1), 172-179. https://doi.org/10.15575/biodjati.v8i1.23764

Xin, K., Guo, R., Zou, X., Rao, M., Huang, Z., Kuang, C., Ye, J., Chen, C., Huang, C., Zhang, M., Yang, W., & Cheng, J. (2023). CO_2 gradient domestication improved high-concentration CO2 tolerance and photoautotrophic growth of *Euglena gracilis*. *Science of the Total Environment, 868*, 161629. https://doi.org/10.1016/j.scitotenv.2023.161629

Xin, Y., Wu, S., Miao, C., Xu, T., & Lu, Y. (2024). Towards lipid from microalgae: Products, biosynthesis, and genetic engineering. *Life, 14*(4), 447. https://doi.org/10.3390/life14040447

Xu, Y., Ibrahim, I. M., & Harvey, P. J. (2016). The influence of photoperiod and light intensity on the growth and photosynthesis of *Dunaliella salina* (Chlorophyta) CCAP 19/30. *Plant Physiology and Biochemistry, 106*, 305-315. https://doi.org/10.1016/j.plaphy.2016.05.021

Yadav, K. K., Musavi, S. F., & Balakrishnan, R. M. (2013). CO2 sequestration and growth characteristics of *Euglena gracilis* in a photo bioreactor. *International Journal of Engineering Research & Technology, 2*(11), 4162-4168. https://doi.org/10.17577/IJERTV2IS110415

Yasuda, K., Nakashima, A., Murata, A., Suzuki, K., & Adachi, T. (2020). *Euglena gracilis* and beta-glucan paramylon induce Ca2+ signaling in intestinal tract epithelial, immune, and neural cells. *Nutrients, 12*(8), 2293. https://doi.org/10.3390/nu12082293

Young, K. E., Quinn, S. M., & Trumble, S. J. (2012). Comparing gas chromatographic techniques used in fatty acid profiling of northern fur seals (*Callorhinus ursinus*) and Steller sea lions (*Eumetopias jubatus*) from Lovushki Island Complex, Russia. *International Journal of Applied Science and Technology, 2*(9), 11-21.

Yuan, A., Sui, F., Li, S., Liu, Y., Lu, X., Lu, Y., & Fan, Y. (2024). Transcriptome analysis of the effects of different carbon dioxide concentrations on paramylon accumulation in *Euglena gracilis* Z. *Bioresource Technology, 393*, 130114. https://doi.org/10.1016/j.biortech.2023.130114

Zhu, Z., Sun, J., Fa, Y., Liu, X., & Lindblad, P. (2022). Enhancing microalgal lipid accumulation for biofuel production. *Frontiers in Microbiology, 13*, 1024441. https://doi.org/10.3389/fmicb.2022.1024441

Zulu, N. N., Zienkiewicz, K., Vollheyde, K., & Feussner, I. (2018). Current trends to comprehend lipid metabolism in diatoms. *Progress in Lipid Research, 70*, 1-16. https://doi.org/10.1016/j.plipres.2018.03.001